RESEARCH ARTICLE | MAY 02 2023

Study of longitudinal mechanisms and correlations in the definition of RFQ transverse acceptance

G. R. Montoya-Soto ; A. M. Lombardi ; G. Bellodi ; C. A. Valerio-Lizarraga ; G. H. I. Maury Cuna

AIP Advances 13, 055105 (2023)
https://doi.org/10.1063/5.0145935

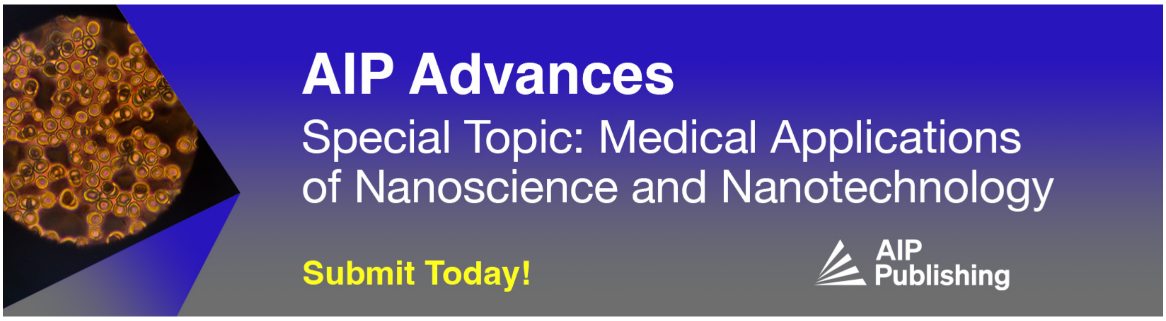

Study of longitudinal mechanisms and correlations in the definition of RFQ transverse acceptance

Cite as: AIP Advances 13, 055105 (2023); doi: 10.1063/5.0145935
Submitted: 13 February 2023 • Accepted: 6 April 2023 •
Published Online: 2 May 2023

G. R. Montoya-Soto,[1,a)] A. M. Lombardi,[2] G. Bellodi,[2] C. A. Valerio-Lizarraga,[3] and G. H. I. Maury Cuna[1]

AFFILIATIONS

[1] Universidad de Guanajuato, León, Guanajuato 37150, Mexico
[2] European Organization for Nuclear Research (CERN), Meyrin, Geneva 1211, Switzerland
[3] Universidad Autónoma de Sinaloa, Culiacán, Sinaloa 80000, Mexico

[a)] Author to whom correspondence should be addressed: gaspar.ricardo.montoya.soto@cern.ch and grmontoya@ugto.mx

ABSTRACT

The Radio Frequency Quadrupole (RFQ) is a linear accelerator that focuses, bunches, and accelerates a continuous input of charged particles while preserving the beam emittance. This paper focuses on the study of the transverse acceptance of an RFQ and how this concept can be used in the design of frontend structures. A simple and fast system to qualify a source and low energy transfer line has been developed in terms of the number of particles delivered in the RFQ acceptance. Multi-particle simulation results show a dependence of the RFQ transverse acceptance on the particle phase in the radio frequency period. The usually referred-to acceptance value is, in fact, just an average value over the 360° phase range, whereas a modulation has been found between more and less favorable phase values, with different patterns depending on the specific structure. We use as a study case three RFQs designed and operated at CERN to investigate such correlations.

I. INTRODUCTION

In hadron linear accelerators (Ref. 1, pp. 2–4), the first acceleration stage is the most critical one due to high beam divergence (Ref. 2, pp. 368–375), large transverse size, space charge effects (Ref. 2, pp. 720–727), and un-bunched particle distribution in the longitudinal plane. Accelerating the beam while maintaining high transmission and beam quality is a challenging scientific and technological problem.[3,4]

As the first acceleration stage in hadron Linacs, Radio Frequency Quadrupoles (RFQ)[5] have reduced the size of the accelerators, increased the transmitted beam current, and accelerated to higher energies than their predecessors[6,7] because of their combined capacity to bunch particles, providing transverse focusing and accelerating the beam while preserving the emittance, all through the same structure that is typically less than 4 m in length.[3,4,8,9]

A modern RFQ is typically divided into four sections (Ref. 1, pp. 232–281): the radial matching section, the shaper, the gentle buncher, and the accelerating section.

The radial matching section adapts a continuous beam to a time-dependent focusing channel, after which the particles travel through an initial slow bunching section called the shaper section where the longitudinal emittance is formed. The acceleration starts smoothly at the gentle buncher section, where the beam bunch reaches its minimum phase spread. Finally, the beam energy increases linearly with longitudinal distance in the accelerating section until the beam exits the RFQ (Ref. 10, pp. 108–113 and Ref. 11)

The RFQ acceptance bottleneck is located at the transition between the gentle buncher and the accelerator where the aperture is at a minimum. This cell, called the critical cell, is typically located at 2/3 of the final length (Ref. 10, pp. 108–110). The transverse acceptance at the critical cell is chosen as a compromise between the maximum field on the vane tips, RFQ length, and final longitudinal emittance. In the case of space-charge-dominated beams, the rate of bunching is also adapted to the transverse phase advance in order to avoid emittance growth due to coupling between the transverse and longitudinal planes.

The RFQ transverse acceptance is defined as the area in phase space (xx' and yy') at the entrance of the RFQ covered by the particles that can be transferred and accelerated. Such an area typically has an elliptical shape given by $A = \pi\varepsilon$, with the orientation of the ellipse matched to the chosen RFQ focusing force and phase advance and described in terms of the Twiss parameters γ, α, and β, (Ref. 2, pp. 213–236).

The RFQ transverse acceptance can be expressed in terms of ε, γ, α, and β values. There is no equivalent definition for the longitudinal acceptance since the beam is continuous at the RFQ input; the quality factors in this case are limited to the average energy and energy spread. As will be shown in this paper, there is, nevertheless, a coupling between the transverse and longitudinal planes, with variations in the transverse acceptance along the RF period.

At the input of the radial matching section, the beam must satisfy specific transverse properties described by the Twiss parameters, which depend on the beam current and the RF electric field: the RFQ acceptance decreases for higher beam current and increases as a function of the RF electric field. The beam properties required to match the beam to the RFQ input must be provided by the source and the Low Energy Beam Transport (LEBT) section: an emittance smaller than the acceptance is desired in order to reduce the beam halo and particle losses (Ref. 10, pp. 108–110).

It is possible to qualify a Source + LEBT frontend performance in terms of the number of particles delivered in the RFQ acceptance with a relatively simple diagnostic device known as an acceptance box.[12] This consists of a system of four plates located within a drift space that allows for ~±120° zero current beam phase advance around a waist. In our case, the plates have square aperture restrictions to cut the beam both horizontally and vertically, thus reproducing the symmetric transverse acceptance of the RFQ. A downstream Faraday cup is used for beam transmission measurements. The particles that pass through the four apertures are the ones that fall within the transverse acceptance of the RFQ. A transverse view of the acceptance box used at the Linac4 source test stand at CERN is shown in Fig. 1, together with a picture of one of the installed plates.[12]

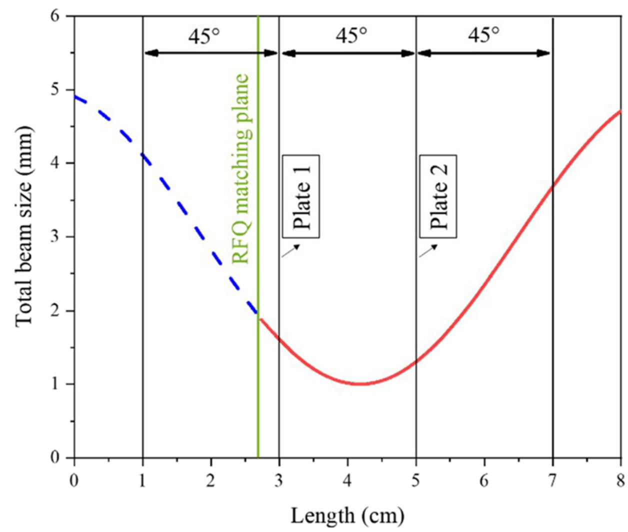

FIG. 2. Representation of the beam size evolution inside the acceptance box: before the matching plane (blue dashed line) and after the matching plane (solid red line). The RFQ matching plane and the blades are represented with perpendicular lines, green and black, respectively.

The plates are installed around the RFQ matching plane such that Plate 1 is located at a distance corresponding to 22.5° phase advance before the minimal beam size and Plate 2 is 22.5° after it. Two additional plates are placed at 45° phase advance upstream of Plate 1 and 45° phase advance downstream of Plate 2, such that the plate cuts are uniformly distributed around the ellipse (see the schematic layout in Fig. 2). The aperture of the plates is defined by the transverse dimensions of the beam at their location.

The comparison between the acceptance of the Linac4 test stand box and the Linac4 RFQ is shown in Fig. 3. The areas of the two acceptance ellipses are very similar, with the beam of the acceptance box being slightly bigger. The orientation of the ellipses is

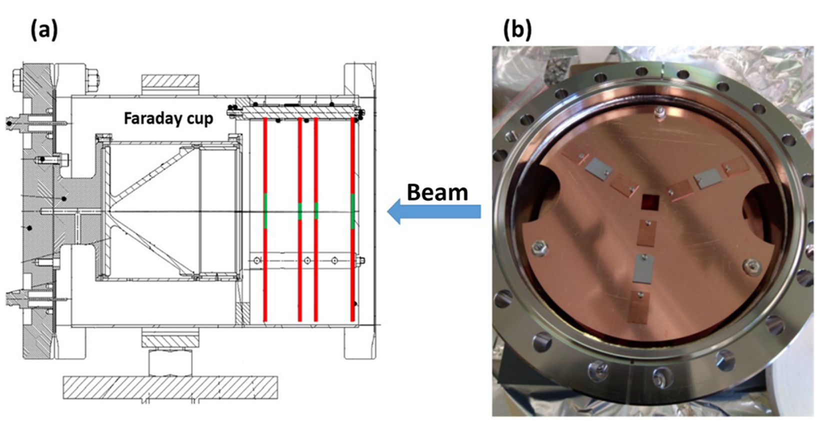

FIG. 1. (a) Linac4 test stand acceptance box layout. The four plates are in red with rectangular holes in green (not on scale). The Faraday cup is located downstream of the plates. (b) A picture of one plate mounted in the acceptance box where the rectangular aperture is visible.

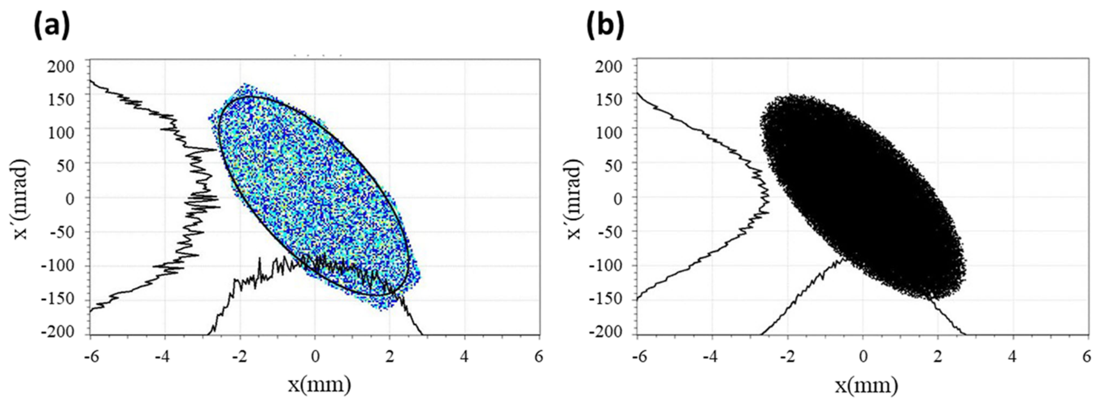

FIG. 3. Comparison between the transverse acceptance of the acceptance box (a) and Linac4 RFQ (b) at zero current.

also in very good agreement. Despite the nearly identical machine layouts in the two setups, transmission measurements through the acceptance box at the Linac4 source test stand have repeatedly shown higher transmission values than measurements at the Linac4 RFQ taken for the same input beam currents. Measurements through the acceptance box overestimate the transmission through the Linac4 RFQ by 15% at 40 mA beam current. Agreement between the two improves for low currents and worsens for high currents (see Fig. 4).[13]

This discrepancy can be explained by the fact that the acceptance box only reproduces the transverse losses and does not take into account the effects of longitudinal mechanisms during the bunching and acceleration processes.[12]

The focus of this paper is to study the correlation that develops between longitudinal and transverse planes in the transport of a beam through an RFQ. The study aims to establish a methodology to qualify a source plus LEBT frontend in terms of the number of particles delivered in the matched RFQ acceptance and hence in terms of its suitability to a given RFQ.

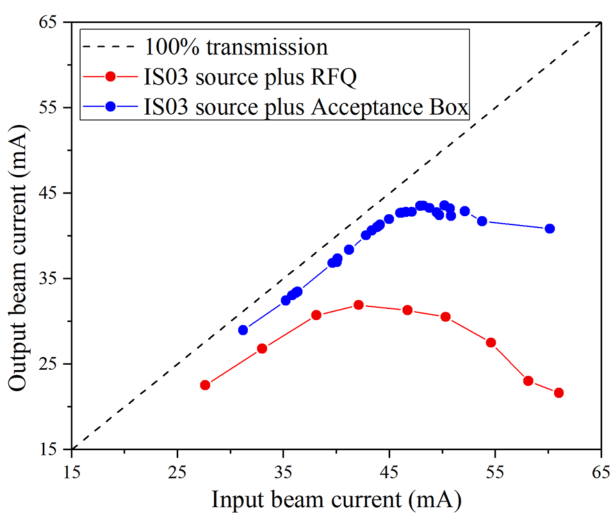

FIG. 4. Beam current measurement comparison after the RFQ (red points) and after the acceptance box (blue points) as a function of the input beam current. The black dashed line represents 100% transmission.

TABLE I. Main parameters of the RFQs studied.

Parameter	Linac4	Linac3	ELISA
Input energy (keV/u)	45	2.5	20
Output energy (MeV/u)	3	0.25	2
RF frequency (MHz)	352.2	101.28	750
Particle species	H^-	$^{208}Pb^{29+}$	p
Design current (mA)	40	0.20	>0.005
Length (m)	3.06	2.5	1
Transmission (%)	≈80[a]	≈80[a]	20[b]
Design vane voltage (kV)	78	70	35
Minimum aperture (mm)	1.77	2.96	0.71
Maximum modulation	2.416	2.055	2.825

[a]Measured at operational configuration.
[b]Expected.

The methodology was tested on three RFQs with differing internal structures installed at CERN[14] in the linear accelerators Linac4,[15–17] Linac3,[18–22] and ELISA.[23,24] The main parameters are listed in Table I.

II. SIMULATION TOOLS AND METHOD

The software used for simulations was Path Manager,[25] whose features include the ability to track particles in the presence of space charge effects and through electromagnetic field (EMF) maps. The EMF maps for each RFQ were generated in Parmteq[26] such that the modulated aperture due to the vanes profiles is included. If not specified, the beam particle distribution plots shown in this paper correspond to the Linac4 case.

In order to determine the RFQ acceptance, the starting point was to create a uniform particle distribution adapted for each RFQ under study, with more than five million particles, extending in x/y over the maximum RFQ aperture, in x'/y' over the maximum accepted angle (such that the transverse emittance is five times larger than the nominal rms value). In the longitudinal plane, the beam spans over 360° simulating a continuous beam, and the energy is equal to the nominal input beam energy with energy spread small enough so as not to influence the results (less than 0.3% variation on the nominal energy). This particle distribution is called the input beam for the first iteration and is shown in Fig. 5. The red lines represent the projections of the particle distribution along each plane and the color scale represents the density of particles.

This *input beam for first iteration* is tracked through the corresponding RFQ field map at zero current. The maximum transverse

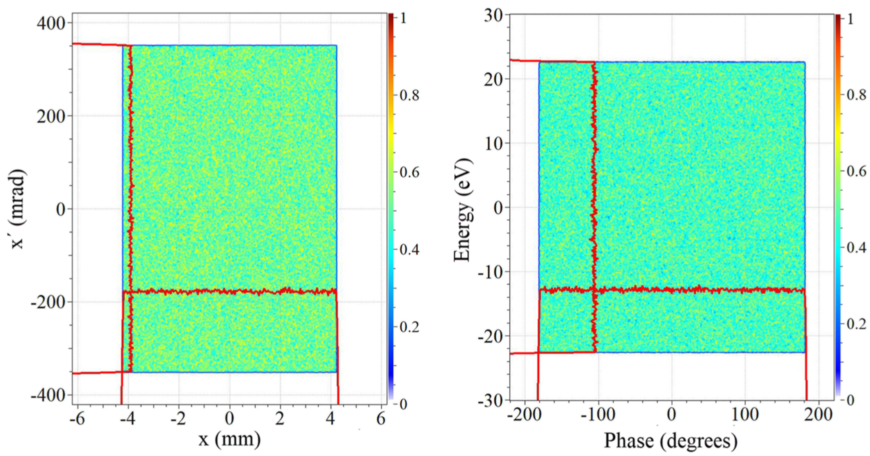

FIG. 5. *Input beam for first iteration* particle distribution and projections. Left: transverse *xx′* (analogous for *yy′*) plane; right: longitudinal *φ–dE* plane.

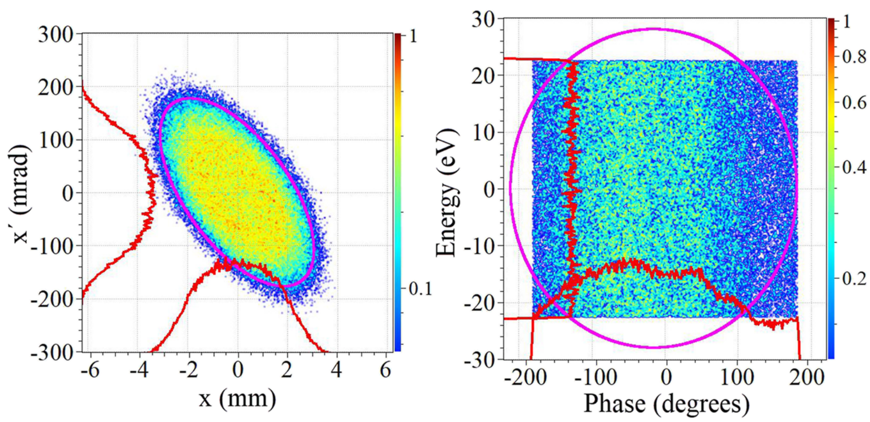

FIG. 6. Beam particle distribution of the *maximum accepted beam* in *xx′* (left), and analogous for *yy′*, and *φ–dE* (right) planes.

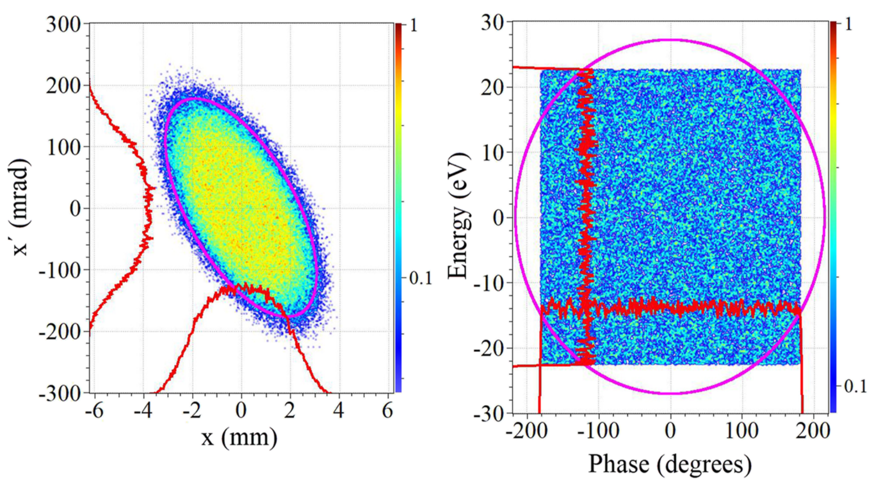

FIG. 7. *Input beam for second iteration.* The transverse plane retains the maximum accepted emittance but is now uniformly distributed in the longitudinal plane.

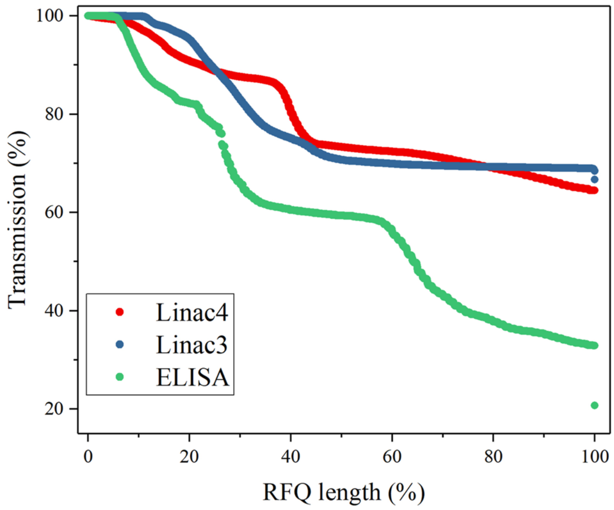

FIG. 8. Transmission behavior for the *input beams for second iteration* through the three RFQ studied.

TABLE II. Comparison of the Twiss parameters in the xx' plane of the *maximum accepted beam* (beam 1) vs *accepted beam* (beam 2).

Parameter	Beam	Linac4	Linac3	ELISA
Emittance (mm mrad)	1	0.91	0.27	0.063
	2	0.73	0.22	0.049
Beta (mm)	1	0.022	0.03	0.01
	2	0.022	0.03	0.01
Alpha (no units)	1	0.76	1.05	0.47
	2	0.77	0.02	0.45
Change in emittance (%)		79.8	18.5	22.3

acceptance of the RFQ is then defined as the input emittance of the particles that are 100% transmitted and accelerated through the RFQ, i.e., the *maximum accepted beam* (as shown in Fig. 6). In these plots, a magenta ellipse covering 90% of the particle population is shown. The *maximum accepted beam* is more densely populated around the center, is phase modulated, and shows no energy spread dependence.

To study the coupling between longitudinal and transverse planes, the longitudinal distribution of the *maximum accepted beam* was regenerated to be uniform, while keeping the transverse planes untouched (see Fig. 7). The beam with the modified longitudinal distribution is named the *input beam for second iteration*. Tracking the beam for zero beam current with the regenerated longitudinal particle distribution through the RFQs proved the influence of longitudinal mechanisms on the transverse acceptance as will be described in Sec. III.

III. RESULTS

Figure 8 presents the transmission for the *input beam for second iteration* through the three RFQs studied. The resulting beam losses are direct evidence of the correlation between the transverse position and longitudinal phase position of the particles. The distance that the beams travel through the RFQ is normalized to the total RFQ length. An energy filter that cuts out particles with an energy less than 85% of the expected output energy is applied at the end of the RFQ. In all three RFQs, the transmission starts to decrease after the radial matching section and continues to decrease at different rates until the exit of the RFQ. The losses associated with a longitudinal mechanism were simulated to be 35.5% for Linac4, 33.3% for Linac3, and up to 79.3% for ELISA. The low energy tails at the RFQ exit were found to be 0% for Linac4, 2% for Linac3, and 12.2% for ELISA.

The reduction in transmission implies a change in the accepted Twiss parameters of the beam. Table II gives the comparison of the Twiss parameters of the *maximum accepted beam* vs the *accepted beam* for the three RFQ structures. Without loss of generality, the values presented refer to only to the xx' plane. The reduction in transmission implies a reduction in the accepted beam emittance of around 20% for all the RFQs, with changes to the beta and alpha Twiss parameters found to be less than 5%.

Figure 9 shows the *accepted beam* particle distribution in the phase–energy plane for the three RFQ structures. The projections onto the horizontal axis in conjunction with the density colors

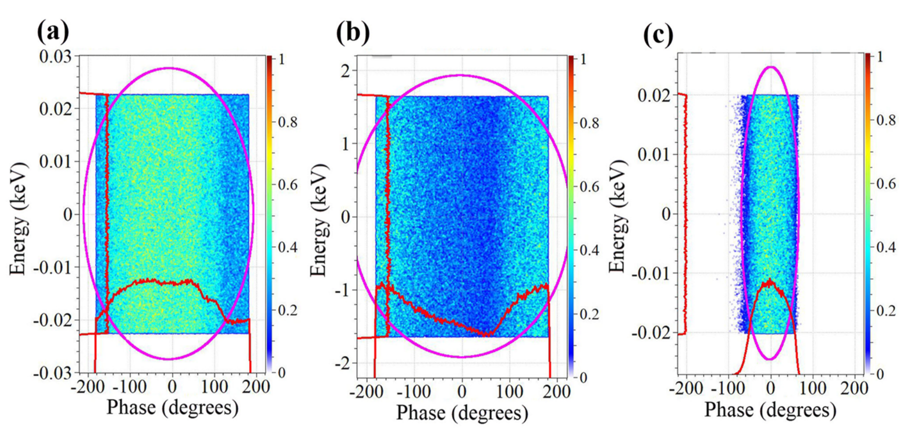

FIG. 9. *Accepted beam* particle distribution in the longitudinal plane with projections. (a) Linac4. (b) Linac3. (c) ELISA.

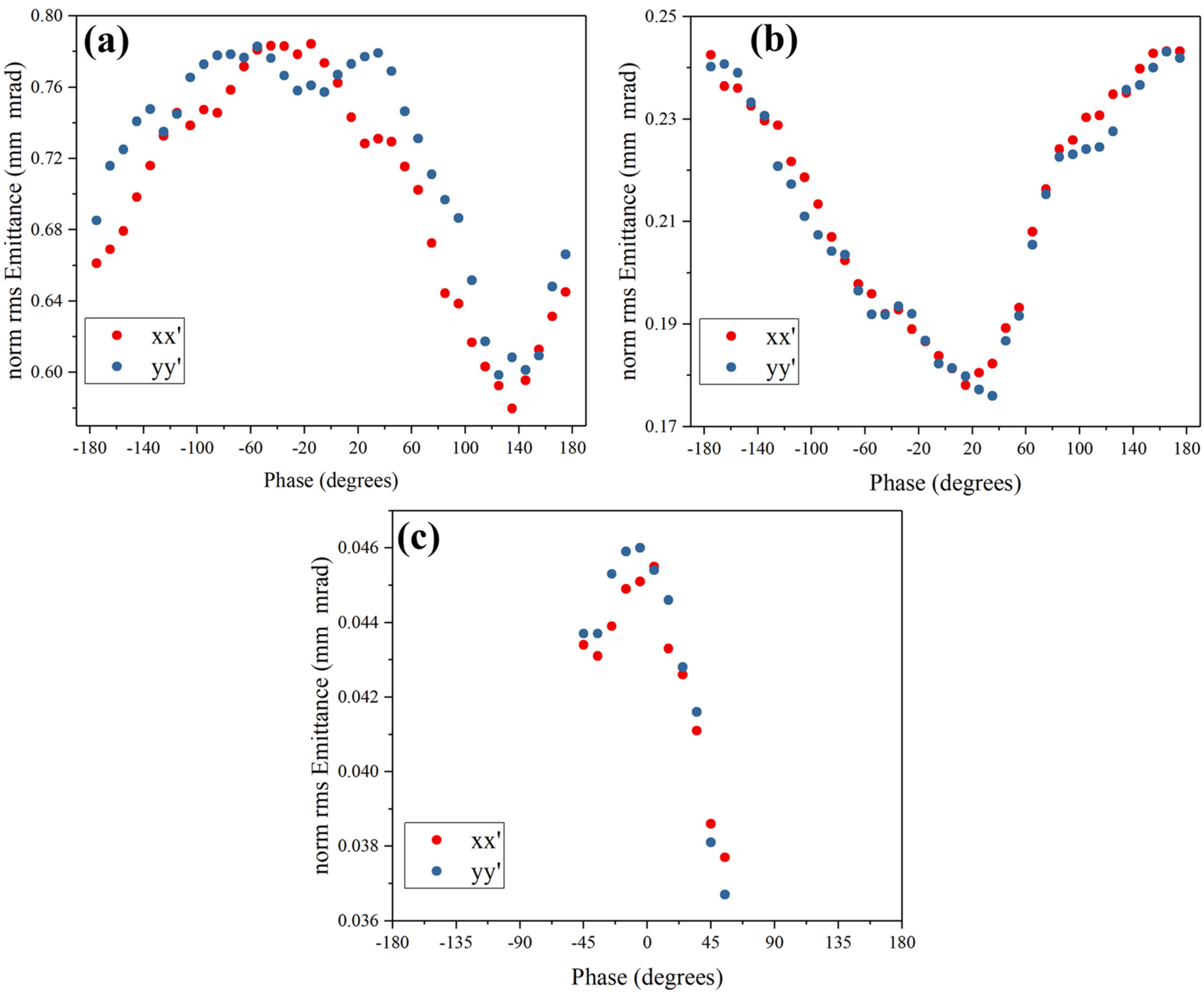

FIG. 10. Phase-dependent transverse acceptance for (a) Linac4, (b) Linac3, and (c) ELISA.

show that the *accepted beam* is longitudinally modulated in phase. In Linac4 and Linac3, particles are captured over 360°, whereas in ELISA, the acceptance is only from −60° to 60° (implying that for a continuous beam, the transmission in ELISA can at maximum be ≈33%). Vertical projections show a uniform distribution in energy spread, showing that this parameter does not influence the results.

To study this correlation in more detail, the input *accepted beam* particle distribution was divided into different phase slices of 10° width, with the RFQ transverse acceptance calculated for each slice (see Fig. 10). The plots show the normalized rms emittance in the transverse planes of the *accepted beam* per phase slice. The three RFQs present similar trends in the horizontal and vertical planes. The reduction in the transverse emittance with respect to the maximum value is between 24% and 28% for Linac4 and Linac3, whereas for ELISA, the reduction is between 15% and 17% over the accepted phase range.

The RFQ vane voltage was then changed to study its influence on the RFQ acceptance. Figure 11 shows the variation in the number of particles in the *accepted beam* as a function of the applied vane voltage (1.0 being the design voltage reported in Table I). For vane voltages below the design value, acceptance is severely degraded, whereas higher vane voltages can lead to improved acceptance. This improvement was up to 5% at a relative vane voltage of 1.05 for ELISA, up to 8% in Linac3, and 12% in Linac4 at a relative vane voltage of 1.2.

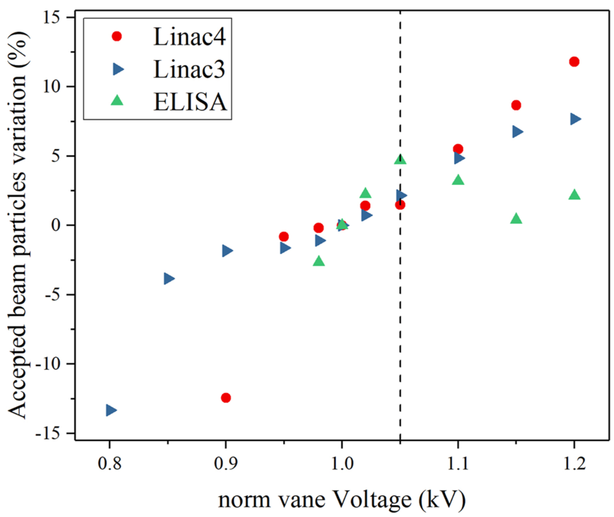

FIG. 11. Variation of the number of particles in the *accepted beam* for Linac4, Linac3, and ELISA for different RFQ vane voltages normalized to the design value. The dashed line at 5% voltage increase represents what could be a realistic change to achieve a gain in transmission with a moderate increase of RF power.

IV. DISCUSSION AND COMPARISON

Despite different design philosophies behind the three structures, all the RFQs studied in this paper present losses due to longitudinal mechanisms. Linac4 is designed to work in high space charge regimes, and for that reason, this RFQ prioritizes strong focusing and acceleration; in Linac3, on the other hand, space charge effects can be neglected due to the low current (0.20 mA), and the structure is tailored to provide the bunch properties required for the next acceleration stage (IH structure). The ELISA case is completely different to the others. This RFQ is designed such that it only accepts particles in a specific longitudinal phase range of 120° and provides acceleration as soon as possible after the radial matching section.

The reduction in the emittance is similar for the three RFQs, with the comparison between the *maximum accepted beam* and the *accepted beam* showing a reduction of about 20% in emittance. The beta and alfa Twiss parameters, on the other hand, remain nearly unchanged.

The accepted beam is modulated in the phase–energy space, thus implying a dependence of the transverse acceptance on the RF phase. While the acceptance can be defined at the most favorable phase, this will lead to an overestimation of the actual acceptance. To be conservative, the least favorable phase value should be considered in the beam dynamics design of the frontend, thus also covering for the unwanted potential effects of factors, such as machining inaccuracies, beam position errors, and space charge effects, which reduce the RFQ acceptance.

Increasing the RFQ vane voltage brings a higher number of particles into the accepted beam due to the enhanced focusing for all beam phases. At first glance, this can be a solution to improve the acceptance; however, in Linac4 and Linac3, the transmission improvement is less than 2% for a 10% power increase. This is, therefore, not a very efficient solution for improving the transmission in Linac4 and Linac3, although it could be an option for ELISA.

V. CONCLUSIONS

Multiparticle simulations carried out on three different RFQ structures have shown that the transverse RFQ acceptance also depends on the longitudinal RF phase. The RFQ transverse acceptance value, as normally quoted, turns out to be close to the average acceptance value across the 360° input beam phase span. This study shows instead that we can define a maximum acceptance as the acceptance at the most favorable phase value and a minimum acceptance as the acceptance at the least favorable phase.

An ideal design of a frontend system composed of Source + LEBT + RFQ is such that the source and LEBT can deliver a matched beam with an emittance smaller than the minimum acceptance. In order to be on the safe side, the least favorable value of the acceptance in its phase modulation should be assumed for the accelerator design.

ACKNOWLEDGMENTS

G. R. Montoya-Soto's doctoral studies were financed by the National Council of Science and Technology (CONACYT for its acronym in Spanish) of Mexico.

Part of this work was supported by the Universidad Autonoma de Sinaloa (Grant No. PRO_A1_022) and by CONACYT (Grant No. CF-2019/2042).

The authors also acknowledge the European Organization for Nuclear Research (CERN) for its human resources and infrastructure.

AUTHOR DECLARATIONS

Conflict of Interest

The authors have no conflicts to disclose.

Author Contributions

G. R. Montoya-Soto: Formal analysis (lead); Methodology (equal); Software (equal); Validation (equal); Writing – original draft (lead); Writing – review & editing (equal). **A. M. Lombardi**: Conceptualization (lead); Methodology (equal); Project administration (lead); Resources (lead); Software (equal); Validation (equal); Writing – original draft (equal); Writing – review & editing (equal). **G. Bellodi**: Methodology (equal); Software (equal); Validation (equal); Visualization (equal); Writing – review & editing (equal). **C. A. Valerio-Lizarraga**: Conceptualization (supporting); Supervision (equal); Validation (equal); Writing – review & editing (equal). **G. H. I. Maury Cuna**: Supervision (equal); Validation (supporting); Writing – review & editing (equal).

DATA AVAILABILITY

The data that support the findings of this study are available from the corresponding author upon reasonable request.

REFERENCES

[1]T. P. Wangler, *RF Linear Accelerators*, 2nd ed. (Wiley-VCH Verlag GmbH & Co. KGaA, 2008), pp. 2–4.
[2]H. Wiedemann, *Particle Accelerator Physics*, 4th ed. (Springer, Cham, 2015).
[3]M. Weiss, "Radio frequency quadrupole," in Proceedings of the CAS-CERN Accelerator School: Accelerator Physics, Geneva, 1987.
[4]M. Vretenar, "The radio-frequency quadrupole," in CAS-CERN Accelerator School: High Power Hadron Machines, Geneva, 2013.
[5]R. H. Stokes, K. R. Crandall, J. E. Stovall, and D. A. Swenson, "RF quadrupole beam dynamics," IEEE Trans. Nucl. Sci. **26**, 3469–3471 (1979).
[6]D. L. Bernard, I. L. Morgan, J. Peoples, B. V. Perrine, and M. C. Taylor, "Pulsed-beam techniques used with a tandem van de Graaff accelerator," in 4th IEEE Particle Accelerator Conference, Chicago, 1971.
[7]G. Reinhold, R. Gleyvod, and K. Trümpy, "High power Cockroft-Walton generator," in 4th IEEE Particle Accelerator Conference, Chicago, 1971.
[8]H. Vormann, A. Schempp, E. Winschuh, H. Liebermann, D. Findlay, J. Hirst, A. Letchford, and G. Murdoch, "RF-tuning of the ISIS-RFQ," in Proceeding of 7th European Particle Accelerator Conference, 2000.
[9]Z. Zhang, S. Cousineaub, A. Aleksandrov, A. Menshov, and A. Zhukov, "Design and commissioning of the Beam Test Facility at the Spallation Neutron Source," Nucl. Instrum. Methods Phys. Res., Sect. A **949**, 162826 (2020).
[10]R. H. Stokes and T. P. Wangler, "Radiofrequency quadrupole accelerators and their applications," Annu. Rev. Nucl. Part. Sci. **38**, 97–118 (1988).
[11]A. M. Lombardi, "The radio frequency quadrupole (RFQ)," in CAS - CERN Accelerator School: Small Accelerators, 2006.
[12]J.-B. Lallement, V. Bencini, S. Bertolo, F. Di Lorenzo, J. Letrry, A. M. Lombardi, C. Mastrostefano, D. Noll, and M. O'Neil, "Activities at the Linac4 test stand," in 29th International Linear Accelerator Conference, 2018.
[13]E. Sargsyan, G. Bellodi, S. Bertolo, F. Di Lorenzo, J. Etxebarria Erdoiza, J.-B. Lallement, A. Lombardi, C. Mastrostefano, and M. O'Neil, Summary of the Linac4 source tests with RFQ1, CERN, 11 May 2022, available at https://indico.cern.ch/event/1140512/contributions/4785885/attachments/2440811/4181224/Summary_of_the_Linac4_source_tests_with_RFQ1.pdf, accessed December 2022 (unpublished).
[14]CERN, https://home.cern/, CERN, 2022, available at https://home.cern/science/accelerators/accelerator-complex/panoramas; accessed December 2022.
[15]C. Rossi, P. Bourquin, J.-B. Lallement, A. M. Lombardi, S. Mathot, M. Timmins, G. Vandoni, M. Vretenar, S. Cazaux, O. Delferriere, M. Desmons, R. Duperrier, A. France, D. Leboeuf, and O. Piquet, "The radiofrequency quadrupole accelerator for the Linac4," in Proceedings of LINAC08, 2008.
[16]C. Rossi, A. M. Lombardi, and A. France, *The Radiofrequency Quadrupole Accelerator for the Linac4, Engineering Specification* (CERN, Geneva, 2009).
[17]M. Vretenar, *Linac4 Design Report*, CERN Yellow Reports: Monographs (CERN, Geneva, 2020).
[18]A. M. Lombardi, G. Parisi, and M. Vretenar, "Comparison study of RFQ structures for the lead ion linac at CERN," in 3rd European Particle Accelerator Conference, 1992.
[19]G. Amendola, J. M. Quesada, M. Weiss, and A. Pisent, "Beam dynamics studies for the CERN lead-ion RFQ," in 3rd European Particle Accelerator Conference, 1992.
[20]M. Comunian and A. Pisent, "Input and output beam matching for a RFQ where a couple of electrodes are at ground potential," in 1994 Linear Accelerator Conference, 1994.
[21]G. P. Bezzon, A. M. Lombardi, G. Parisi, A. Pisent, M. Weiss, P. Bourquin, and M. Vretenar, "Construction and commissioning of the RFQ for the CERN lead-ion facility," in 1994 Linear Accelerator Conference, 1994.
[22]H. Haseroth, "The CERN heavy ion facility," In *Proceeding of 4th European Particle Accelerator Conference* (Cern, 1994).
[23]A. M. Lombardi, V. A. Dimov, M. Garlasche', A. Grudiev, S. Mathot, E. Montesinos, S. Myers, M. Timmins, and M. Vretenar, "Beam dynamics in a high frequency RFQ," in 6th International Particle Accelerator Conference, Richmond, 2015.
[24]M. Marchi, A. Grudiev, S. Mathot, and H. Pommerenke, "RF measurements and tuning of the CERN 750 MHz ELISA-RFQ for public exhibition," in Proceedings of LINAC22, 2022.
[25]A. Perrin, J.-F. Amand, T. Mütze, L. Jean-Baptiste, and S. Lanzone, Travel user manual, Vol. 4.07, CERN, Geneva, 2007.
[26]K. R. Crandall, T. P. Wangler, L. M. Young, J. H. Billen, G. H. Neuschaefer, and D. L. Schrage, "RFQ design codes," Report No. LA-UR-96-1836, 1998.